Cell, Vol. 31, 215–226, November 1982, Copyright © 1982 by MIT

Impulse Responses in Bacterial Chemotaxis

Steven M. Block, Jeffrey E. Segall and Howard C. Berg
Division of Biology
California Institute of Technology
Pasadena, California 91125

Summary

The chemotactic behavior of Escherichia coli has been studied by exposing cells tethered by a single flagellum to pulses of chemicals delivered iontophoretically. Normally, wild-type cells spin alternately clockwise and counterclockwise, changing their direction on the average approximately once per second. When cells were exposed to a very brief diffusive wave of attractant, the probability of spinning counterclockwise quickly peaked, then fell below the prestimulus value, returning to baseline within a few seconds; repellent responses were similar but inverted. The width of the response indicates that cells integrate sensory inputs over a period of seconds, while the biphasic character implies that they also take time derivates of these inputs. The sensory system is maximally tuned to concentration changes that occur over a span of approximately 2 sec, an interval over which changes normally occur when cells swim in spatial gradients; it is optimized to extract information from signals subject to statistical fluctuation. Impulse responses of cells defective in methylation were similar to those of wild-type cells, but did not fall as far below the baseline, indicating a partial defect in adaptation. Impulse responses of *cheZ* mutants were aberrant, indicating a serious defect in excitation.

Introduction

Flagellated bacteria swim in a purposeful manner. They move up gradients of some chemicals (attractants) in search of food and down gradients of other chemicals (repellents) to avoid noxious substances. The cells are propelled by thin, helical flagella, each driven at its base by a reversible rotary motor. The behavioral repertoire of Escherichia coli and Salmonella typhimurium consists of runs and tumbles. During a run, the flagellar filaments rotate in concert in a helical bundle, pushing the cell steadily forward. Each run is terminated by a tumble, during which the filaments change their direction of rotation, the bundle flies apart and the cell moves erratically, with little net displacement. At the end of a tumble, the cell runs again, moving off in a new direction. The direction of rotation of a flagellar motor is determined in part by sensory inputs. In a chemically isotropic environment, changes in the direction of rotation occur at random, and a cell executes a three-dimensional random walk. Run and tumble intervals are each distributed exponentially, with time constants on the order of 1 and 0.1 sec, respectively. In a gradient of an attractant (or repellent) the rotational bias is altered in such a way that runs that happen to carry the cell in a favorable direction are extended. This imposes a drift on the random walk that carries the cell up (or down) the gradient. Temporal changes in concentration experienced by the cell as it moves in a gradient lead to variations in the occupancy of chemoreceptors that, in turn, alter the rotational bias of the flagellar motors. (For recent reviews on bacterial chemotaxis see Macnab, 1978; Springer et al., 1979; Koshland, 1981; Parkinson, 1981; Boyd and Simon, 1982.)

What is the pathway linking the receptors to the flagella? How does it function? While many of the components of this pathway have been identified genetically and some of their biochemical interactions are known, most of the events that occur during signal processing remain obscure. The work reported here defines the physiological properties of the sensory-transduction pathway in detail, both in the wild-type and in certain mutant cells. It is based on a method that provides means for systematic analysis of chemotactic behavior at the level of an individual flagellar motor.

The output of a single motor can be monitored by tethering the flagellar filament to a glass surface (Silverman and Simon, 1974). When the filament is held fixed, the motor spins the cell body alternately clockwise (CW) and counterclockwise (CCW). Rotation in the CCW direction (as viewed from a point in the external medium above the cell) corresponds to the run mode, while rotation in the CW direction corresponds to the tumble mode (Larsen et al., 1974). This preparation is particularly useful for the study of behavior: the cell remains at a fixed position for observation, while the chemical milieu may be changed at will. When properly energized, cells remain active for hours. A tethered cell can be stimulated by mixing in an attractant or a repellent (Larsen et al., 1974), by displacing one medium with another containing an attractant or a repellent (Berg and Tedesco, 1975) or by positioning an iontophoretic micropipette containing a charged attractant or repellent near the cell and passing an electric current (Segall et al., 1982).

The first two methods have been used in studies of adaptation, wherein cells exposed to the sudden addition of a large amount of attractant spin CCW for minutes, spin CW for a somewhat shorter time and then gradually relax to their initial mode of behavior (Berg and Tedesco, 1975). Cells exposed to the sudden removal of attractant spin CW for many seconds, spin CCW for a shorter time and then resume their initial mode of behavior. Similar responses are observed when repellents are removed or added, respectively. The biochemical basis for this adaptive behavior appears to be the reversible carboxymethylation of proteins found in the cytoplasmic membrane called methyl-accepting chemotaxis proteins (MCPs;

Kort et al., 1975). Individual polypeptides are multiply methylated in a sequential fashion, the final steady-state level of methylation reflecting the external concentration of attractant or repellent (Boyd and Simon, 1980; Chelsky and Dahlquist, 1980; DeFranco and Koshland, 1980; Engström and Hazelbauer, 1980). The time course for methylation in response to addition of attractant closely parallels that for physiological adaptation (Goy et al., 1977). When the concentration of an attractant increases (or that of a repellent decreases), methyl groups are added gradually; when the concentration of an attractant decreases (or that of a repellent increases), they are removed rapidly. These steps are catalyzed by two cytoplasmic enzymes: a methyltransferase, the product of the *cheR* gene (Springer and Koshland, 1977), and a methylesterase, the product of the *cheB* gene (Stock and Koshland, 1978); *che* refers to generally nonchemotactic. The MCPs also serve to integrate information from different sets of receptors and to relay that information to the flagellar motors. Accordingly, their genes have been designated *tar* (taxis to aspartate and some repellents), *tsr* (taxis to serine and other repellents) and *trg* (taxis to ribose and galactose) (Silverman and Simon, 1977; Springer et al., 1977; Kondoh et al., 1979).

Several other gene products are involved in signal processing. Direct interactions between some of these components have been demonstrated by reversion analysis and interspecies complementation. For example, the *cheY* gene product interacts with the methyltransferase and with components of the flagellar motor involved in controlling the direction of rotation (the *cheC,* or *flaA,* and the *cheV,* or *flaB,* gene products). The *cheZ* gene product interacts with the methylesterase and with these components of the motor as well. The functions of these and other *che* gene products, such as *cheA* and *cheW,* are not known (see Parkinson, 1981).

The iontophoretic method has been used in studies of excitation, in particular, to measure response latencies (Segall et al., 1982). When cells are exposed to rapid step changes in the concentration of attractants or repellents, responses to these stimuli occur in about 0.2 sec. This is true both for wild-type cells and for cells carrying a *cheR–cheB* double deletion. Response latencies of *cheZ* mutants are much longer. These latencies are relatively insensitive to the magnitude of the stimulus, provided that the change in chemoreceptor occupancy is above the threshold level. The response latency is a measure of the time required for signals to be processed by the complete transduction pathway. Given the small size of the organism, the latency of wild-type cells is surprisingly long, suggesting that the excitation pathway is complex.

There are two serious problems with the studies of tethered cells made thus far. The first is that measurements of adaptation times and response latencies provide only a limited amount of information about the transduction machinery. The second is that the stimuli used are so large that this machinery is driven into saturation; the information that is obtained may not be relevant to the behavior of the cell in the real world, where stimuli are much smaller. Cells swimming in spatial gradients do not experience large temporal stimuli, because discontinuities in concentration are smoothed out by diffusion.

We have used the iontophoretic technique to expose cells to impulsive stimuli rather than to large-step stimuli, and we have followed each cell's behavior for many seconds, not just to the next flagellar reversal. In these experiments, a small amount of chemical is ejected from the micropipette over a period of a few milliseconds. The chemical spreads outwards as a diffusive wave, passing over the tethered cell and rapidly dissipating in the external medium. If the time course of the wave is sufficiently short, it can be treated as an idealized impulse. The behavior of the cell toward this stimulus is an impulse response. Impulse responses have two very useful features. The first is that they reflect only the time constants of processes occurring in the system under study, not the time constants of the stimulus itself. A simple analogy is a bell struck by the percussive impulse of a clapper: a characteristic tone is generated that decays with time. The fundamental frequency of the tone and its rate of decay reflect intrinsic properties of the bell itself, not properties peculiar to the clapper. The second feature is that the impulse response contains all the information necessary to predict the behavior of the system when it is exposed to an arbitrary stimulus. One need only decompose the arbitrary stimulus into a series of impulses of appropriate magnitude and timing and compute the sum of the responses that would be observed, were these impulses applied separately. However, for this computation to work, the stimulus must be small enough that there are no nonlinear effects: the response to each impulse must remain independent of whether or not the cell is still responding to previous impulses (see Papoulis, 1977; Marmarelis and Marmarelis, 1978).

The early events in chemotaxis occur on a time scale of tenths of a second, and cannot be resolved by methods previously used to explore bacterial behavior. The iontophoretic technique has allowed us to generate stimuli that are short enough to be impulsive. By monitoring the rotation of tethered cells with an optoelectronic device accurate to a fraction of a cycle, we have achieved the temporal resolution necessary to characterize the response to these stimuli. The response has properties that imply that the sensory system in E. coli is optimally designed to allow cells swimming in spatial gradients to extract information about changes in concentration from signals subject to statistical fluctuations.

Results

Computation of the Impulse Response

Cells were tethered to a glass window and viewed through the water-immersion lens of a phase-contrast microscope. The microscope was equipped with linearly graded optical filters that extract the x and y coordinates of the centroid of the image of a spinning cell; sensors viewing these filters generate signals that contain information about the cell's angular velocity and direction of rotation. A micropipette was positioned within about 4 μm of the cell, and the cell was stimulated by short iontophoretic pulses, repeated at intervals of about 1 min. Time records of the x and y signals were made on a strip-chart recorder, together with event markers indicating the direction of rotation of the cell and the timing of the stimulus current. The size of the stimulus to which the cell was exposed could be varied by adjusting either the magnitude of the current passed through the pipette or its duration. These parameters were adjusted by hand during the experiment to ensure that responses occurred, but under conditions in which the stimuli were impulsive (see below). Records of 20 sec duration bracketing each iontophoretic pulse were digitized and stored in a computer for subsequent analysis.

The rotational behavior of a tethered bacterium is a binary, stochastic process: it is the probability of spinning CW or CCW that is modulated by the sensory apparatus. Therefore, we took as our measure of the response the probability that a cell spins CCW. We obtained an estimate of this probability by taking the average of a series of records, each containing data obtained with a single stimulus. The procedure is outlined in Figure 1. A typical result obtained with 25 records from a single cell is shown in Figure 2. The fluctuation about the baseline before and after the stimulus results from the averaging of binary signals. Its amplitude obeys the bionomial distribution; the mean amplitude decreases as the inverse square root of the number of records. To verify this fact and to test our data-reduction procedures, we used a Monte Carlo method to construct records of an "artificial cell" whose CW and CCW rotation intervals were given by exponential distributions. These records were processed in the same way as the real data. The probabilities computed from artificial and real data had similar statistical properties, which agreed with theory.

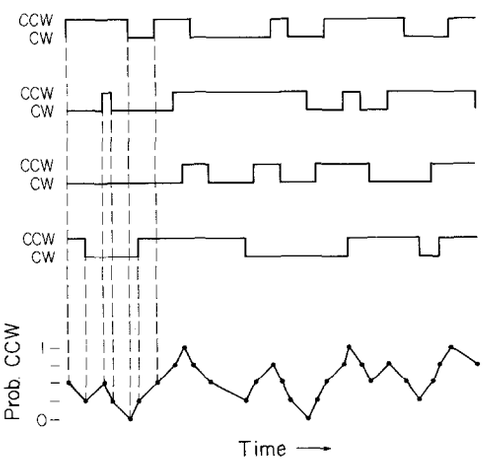

Figure 1. Scheme for Averaging Data Records

Individual binary records of rotational behavior (four are shown) were placed in register at the time of stimulation. A value of +1 was assigned to each record when the direction of rotation was CCW and 0 when it was CW. The average value of these numbers was computed each time a transition (an event) occurred in any one of the individual records. The result (bottom) is a function that can assume any one of $n + 1$ values between 0 and 1 inclusive, where n is the number of records. The value of this function provides an estimate of the probability of CCW rotation, and the density of points along the time axis gives an estimate of the average reversal rate. The algorithm actually used to perform this computation is described in the experimental Procedures.

Impulse Responses of Wild-Type Cells

The impulse response to attractant stimuli is shown in Figure 3A. The same response was observed with aspartate and α-methylaspartate; only the threshold concentrations differed. Prior to stimulation, the directional bias of the cells averaged 64% CCW. After the pulse at time zero (5 sec on the scale shown in the figure), the probability of spinning CCW rose sharply to a maximum value at 0.4 sec, then fell in a smooth manner, crossing the baseline at 1 sec and reaching a minimum value at 1.5 sec, and finally returning to its initial value at approximately 4 sec. The excursion below baseline (the response undershoot) is important, because it implies that the chemosensory system has adaptive properties in the 1 sec time domain (see below). The areas of the two lobes of the response were equal.

The impulse response to repellent stimuli is shown

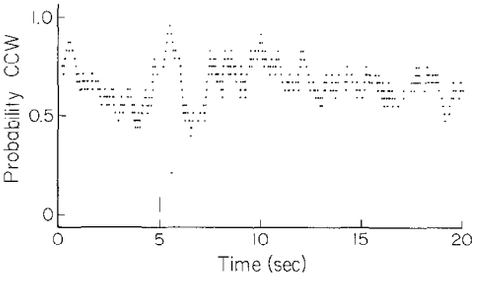

Figure 2. Impulse Response of a Single Cell

A single cell was stimulated 25 times by a pulse given at 5 sec (vertical line). The graph shows the probability of CCW rotation as a function of time, estimated as described in the legend to Figure 1. The pipette contained 100 mM α-methyl-D,L-aspartate, a negatively charged attractant. Pulses were generated by switching the current from 0 to −100 nA for a period of 100 msec. The discrete layer lines that appear in the data are determined by the 26 quantized values obtained when 25 binary records are averaged. Data were not smoothed.

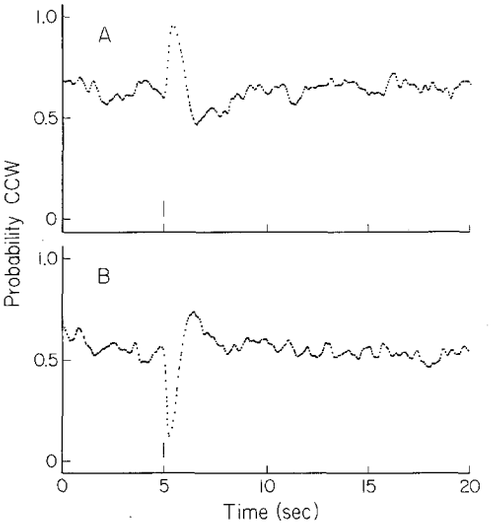

Figure 3. Impulse Responses of Wild-Type Cells

The probability of spinning CCW is shown as a function of time, with stimuli given at 5 sec (vertical line). The data were smoothed, as described in the Experimental Procedures.

(A) Attractant response. The pipettes contained either 1 mM L-aspartate or 7 mM α-methyl-D,L-aspartate. Pulses were generated with currents ranging from −1 to −100 nA switched on for periods of 20–100 msec. The graph was constructed from 172 records containing 3193 events obtained with nine different cells; 399 points are displayed; 115 of the records were from stimulation by L-aspartate, 57 from stimulation by α-methyl-D,L-aspartate.

(B) Repellent response. The experiment was carried out as described in (A), but with pipettes containing 200 mM benzoate or 1 mM L-aspartate. Benzoate was injected at −100 nA for 20–50 msec. L-aspartate was added continuously at −2 to −3 nA, and the addition was interrupted by switching to +3 to +10 nA for 20–40 msec. Addition of repellent or removal of attractant gave the same response. The graph was constructed from 169 records containing 2785 events obtained with seven different cells; 397 points are displayed; 86 of the records were from addition of repellent, 83 from removal of attractant.

in Figure 3B. The responses to the addition of benzoate and to the removal of aspartate were similar. The repellent response resembled an inverted attractant response, with a similar time course and biphasic character. The cells responded to the addition of benzoate and nickel chloride on a slightly shorter time scale than they did to the removal of aspartate (data not shown).

The pulses used represented true impulses, as indicated by the following experimental criteria: pulses were adjusted to be close to, but generally above, threshold for a response; in a trial experiment, stimuli of lower amplitude resulted in a smaller probability of a change in directional bias, but gave an impulse response with the same time course; and cells with different thresholds, exposed to pulses of different amplitude and duration, also gave an impulse response with the same time course. Finally, a theoretical calculation of the diffusive wave (Segall et al., 1982) showed that for the 20–40 msec pulses used with wild-type cells, the change in chemoreceptor occupancy had fallen to less than 3% of its maximum value by 200 msec after the onset of the pulse, long before the end of the response was observed.

As stated above, the impulse response has predictive value when the system operates in a linear domain—that is, when responses to different stimuli add algebraically to give the overall response. In this domain, the response to an arbitrary stimulus is given by the convolution of that stimulus with the impulse response (Papoulis, 1977), a process that decomposes the stimulus into an infinite set of impulses of appropriate magnitude and timing and adds their responses together. For the simple case of the response to a step, the convolution reduces to the integral of the impulse response with time. The extent to which such a convolution predicts the system response is a measure of the linearity. In Figure 4, the measured response of wild-type cells to a small step change in concentration of an attractant is compared with the response predicted by integration of the impulse response; the agreement is satisfactory.

Does the response to an impulse depend on the initial state of the flagellar motor? That is, does it matter in which direction a cell happens to be spinning when it is stimulated? To answer this question, we separated the data into two parts: one containing those records for which the cell was spinning CW at a given instant, and another containing those for which the cell was spinning CCW at that instant. If this is done for an arbitrary time, t_0, the records will be autocorrelated around that time in both directions. For example, if a cell happened to be spinning CCW at time t_0, it is likely that it was also spinning CCW for times close to t_0. For CCW intervals that are distributed as $\exp(-k_r t)$ and CW intervals distributed as $\exp(-k_t t)$, where k_r and k_t are the run and tumble rate constants, respectively, the autocorrelation function decays as $\exp[-(k_r + k_t)|t - t_0|]$. This effect is seen in Figure 5A. Both curves decay symmetrically to the baseline with similar time constants. The small difference in baseline for the two curves is a reflection of the fact that records chosen for cells that happen to be spinning in a given direction at an arbitrary time are more likely to belong to cells that are generally biased in that direction. If, however, the time t_0 is chosen to coincide with the time of the pulse, an intriguing result is obtained, as seen in Figure 5B. The two curves are back-correlated, as in Figure 5A, but now they follow an identical time course once cells that were spinning CW have had time to change their direction of rotation—that is, after an interval equal to the response latency. (The somewhat larger disparity in baselines for Figure 5B relative to Figure 5A also reflects the way in which the records were chosen, and is not statistically significant.) This implies that the response does not depend on the initial state of the

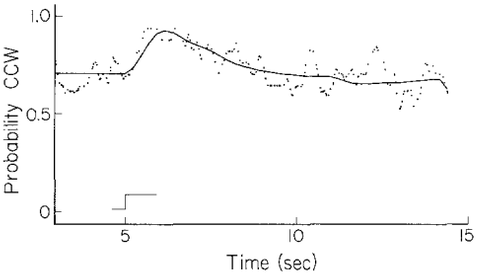

Figure 4. Small-Step Response of Wild-Type Cells

The probability of spinning CCW is shown as a function of time, with stimuli given at 5 sec (step mark). The data were smoothed, as described in the Experimental Procedures. The response to a small step increase in concentration of attractant (dotted line) is compared with the response predicted from integration of the impulse response (solid line). The pipette contained 0.1 mM L-aspartate. Steps were generated by switching the current from 0 to a value of −3 nA and maintaining that value for at least 10 sec. The experimental probability function was constructed from 34 records containing 417 events obtained with a single cell; 209 points are displayed. The impulse response was integrated from the beginning of the step onward in accordance with the convolution theorem (see text). The choices of baseline and amplitude for the predicted curve are arbitrary; they were scaled to match the baseline and amplitude of the experimental data. The impulse response used was similar to that shown in Figure 3A. It was derived from 237 records containing 4585 events obtained with 11 different cells.

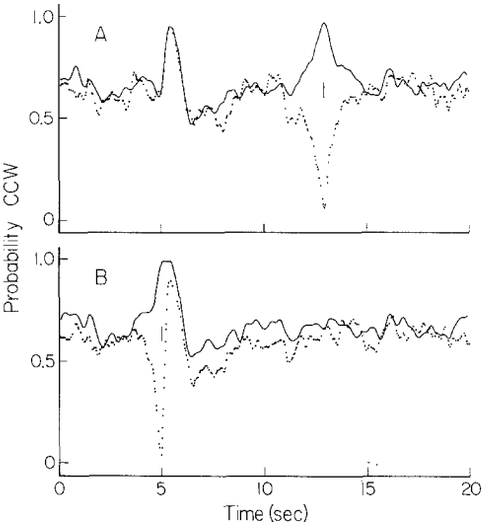

Figure 5. Stimulation during Either a CCW or a CW Interval

(A) The individual records used to compute Figure 3A were separated into two groups: those for cells that were rotating CCW (solid line) 8 sec after the pulse (at 13 sec; vertical line), and those that were rotating CW (dotted line). These groups were averaged separately to yield the graphs shown. The probability of being in the CCW or the CW mode is unity at 13 sec and decays exponentially in either direction to the baseline, as determined by the autocorrelation function (see text).

(B) The same records were separated into two different groups: those for cells that were rotating CCW (solid line) at the time of the stimulus pulse (5 sec; vertical line), and those that were rotating CW (dotted line). Both probabilities decay backwards in time, as in (A), but now the curves are nearly identical for times greater than 5.2 sec—that is, after an interval equal to the response latency.

motor, and that the mechanism responsible for the impulse response overrides the mechanism that generates spontaneous reversals.

Reversal Rate during Impulse Responses

As noted in the legend to Figure 1, the density of points along the time axis of the probability function provides an estimate of the average reversal rate. Such an estimate is shown in Figure 6, together with the repellent response from which it was derived. Once again, fluctuations around the baseline reflect the underlying statistical process; here, the amplitude of the fluctuations obeys a distribution related to the Poisson distribution, with a characteristically large variance. During the initial phase of the response, the reversal rate rose sharply, to a value of greater than 3 reversals/sec/cell, a consequence of the fact that cells that happened to be spinning CCW at the time of the pulse changed their direction of rotation within a narrow time interval. Shortly after the response minimum, the reversal rate fell to its lowest value, of approximately 0.3 reversals/sec/cell: the reversal rate is actively supressed during the response. A subsidiary peak in the reversal rate occurred during the overshoot, whereafter the rate returned to its initial value. Reversal rates for attractant responses were nearly identical, but showed a somewhat less pronounced initial peak (1.5 reversals/sec/cell; data not shown). We will return to these data later when we discuss the two-state system (see Discussion).

Impulse Responses of Mutant Cells

The impulse response was determined for several generally nonchemotactic mutants, provided by J. S. Parkinson. Where possible, mutants with nonpolar deletions were used to ensure the null phenotype. The attractant response of cells carrying *cheR–cheB* double deletions is shown in Figure 7A. These mutants lack genes for both the methyltransferase and the methylesterase; they are defective in adaptation. Nevertheless, they have about the same directional bias as the wild-type and respond to large-step stimuli. Their impulse response was similar to that of the wild-type (Figure 3A); however, the initial peak was longer, and the undershoot was substantially smaller, in the mutant cells. The degree of undershoot varied from cell to cell; when examined individually, the cells whose average response is shown in Figure 7A showed different degrees of undershoot, ranging from none at all to a size comparable with that of the wild-type.

Mutants in *cheZ* have a large CW bias, high response thresholds and abnormally long response latencies (Parkinson, 1978; Parkinson and Parker, 1979; Segall et al., 1982). Very short impulses of L-aspartate failed to produce a response; however,

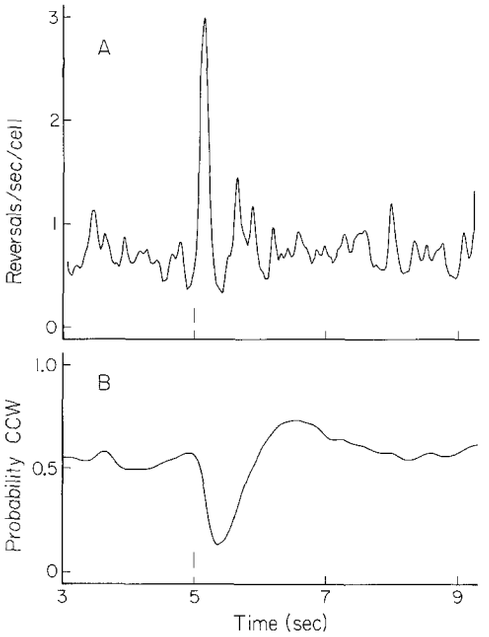

Figure 6. Reversal Rate during the Impulse Response

(A) The instantaneous reversal rate for cells undergoing an impulse response, plotted as a function of time. Note the expanded time scale. The reversal rate was calculated from the density of points along the time axis in the data summarized in Figure 3B.

(B) The curve of Figure 3B, shown on the same expanded time scale for comparison. Data were smoothed.

somewhat longer pulses proved effective, with the result shown in Figure 7B. The response latency was highly variable, ranging from 0.2 sec up to 5 sec or more. Typically, a cell changed its direction of rotation from CW to CCW after a relatively long (but variable) latency, spun CCW for a period of less than a second and then exhibited a few brief CCW intervals over the next 5 sec, before returning to its initial (CW) behavior. In some cases, responses continued over a much longer time period. Note (Figure 7B) that the response failed to return to baseline even 15 sec after the pulse. The low peak probability for CCW rotation apparent in the figure arose for the following reasons: some cells responded to every pulse, but with a variable time course, so that peak responses failed to add together in phase; and some cells responded with a probability less than unity—they continued to respond over the course of the experiment, but not to every pulse.

Mutants with *cheB* deletions are missing the methylesterase; they have a large CW bias and very high response thresholds (Parkinson, 1978; Sherris and Parkinson, 1981). Mutants with *cheR* deletions are missing the methyltransferase; they have a large CCW bias and high response thresholds (Goy et al., 1978; Parkinson and Revello, 1978). The responses of these mutants to attractants and repellents are shown in Figures 7C and 7D, respectively. These responses resembled those observed for the wild-type; in each case, the initial peak had a similar time course. The

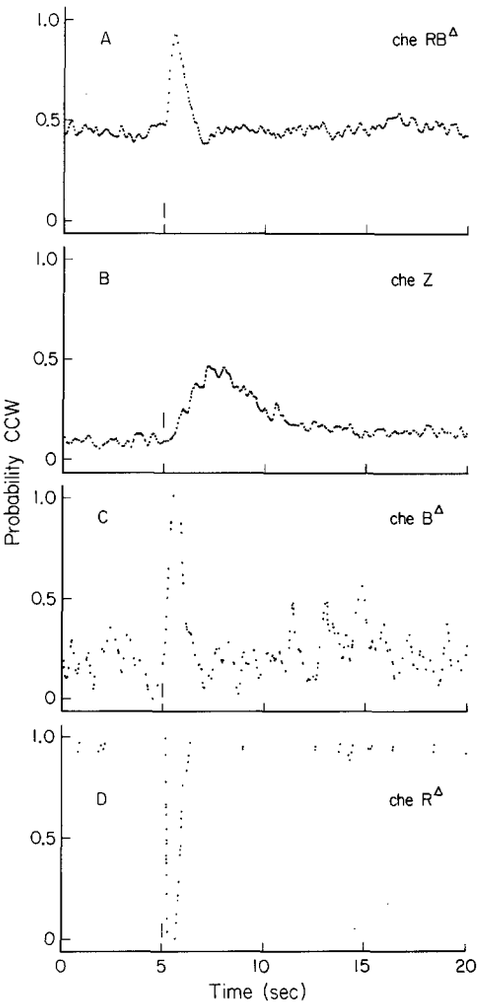

Figure 7. Impulse Responses of the *che* Mutants

The probability of spinning CCW is shown as a function of time, with stimuli given at 5 sec (vertical lines). The data have been smoothed, as described in the Experimental Procedures.

(A) Attractant response of cells carrying *cheR–cheB* double deletions. Pipettes contained 10 mM L-aspartate. Pulses were generated with currents ranging from −20 to −100 nA switched on for periods of 9–225 msec. The graph was constructed from 167 records containing 4260 events obtained with 11 different cells; 335 points are displayed.

(B) Attractant response of the *cheZ* point and amber mutants. Pipettes contained 1 mM L-aspartate. Pulses were generated with currents of −10 to −100 nA switched on just long enough to give a response (0.2–1.8 sec). The graph was constructed from 132 records containing 2034 events obtained with five different cells; 339 points are displayed.

(C) Attractant response of a cell carrying a *cheB* deletion. Pipettes contained 100 mM L-aspartate. Pulses were generated with a current of −100 nA switched on for 200–300 msec. The graph was constructed from 14 records containing 248 events obtained with a single cell. The mutant was CW-biased; noise in the baseline arose from occasional spontaneous reversals.

(D) Repellent response of a cell carrying a *cheR* deletion. Pipettes contained 100 mM nickel chloride. Pulses were generated with currents of +2 nA switched on for 20 msec. The graph was constructed from 19 records containing 63 events obtained with a single cell. The mutant was CCW-biased; points on the baseline represent rare spontaneous reversals.

greater amplitude of this peak and the lack of undershoot (or overshoot) in the mutant cells may simply reflect the altered range available for changes in directional bias. A run-biased *cheR* point mutant (*cheR202*) gave a similar response to the *cheR* deletion mutant (data not shown). Mutants in *cheB* proved extremely hard to excite: only a small fraction of the cells responded reproducibly to stimulation by L-aspartate, even with relatively high concentrations in the pipette.

The records for the *cheR–cheB* and *cheZ* mutants were separated into two groups: those corresponding to cells that were stimulated while spinning CW, and those that were stimulated while spinning CCW. Although the probability functions differed from mutant to mutant (data not shown), it was clear in these mutants, as well as in the wild-type (Figure 5), that the mechanism determining the response to an impulse overrides the mechanism that generates spontaneous reversals.

Discussion

A conceptual distinction has been drawn in bacterial chemotaxis between excitation and adaptation (Goy et al., 1978; Springer et al., 1979). While the addition of an attractant or repellent causes an almost immediate response (excitation), that response gradually disappears with time, even if the attractant or repellent is still present (adaptation). In most cases, adaptation is complete: the behavior of the cell does not depend on the ambient concentration after a sufficiently long period of time (Macnab and Koshland, 1972; Tsang et al., 1973). There are some exceptions: for example, when cells in motility medium are exposed to serine (Berg and Brown, 1972), or when enough weak acid is added to cells in an acidic medium to perturb seriously the cytoplasmic pH (Kihara and Macnab, 1981). For the relatively large stimuli used in previous work, the time required for a cell to respond (the response latency) is about 0.2 sec (Segall et al., 1982). However, the time required for a cell to adapt (the adaptation time) ranges from several seconds to several minutes, depending on the magnitude of the change in receptor occupancy (Spudich and Koshland, 1975; Berg and Tedesco, 1975). These characteristic times are so different as to suggest that the pathways for excitation and adaptation are distinct. This notion is supported by the observation that cells carrying mutations in the *cheR* gene have normal response latencies (Segall et al., 1982) but fail to adapt (Goy et al., 1978; Parkinson and Revello, 1978). Alternatively, the disparity in characteristic times for excitation and adaptation might be an artifact of the step–stimulus paradigm, in which a large change in concentration rapidly drives the system into saturation. Measurements of the impulse response have allowed us to characterize the behavior of cells in the small-signal domain. Our results suggest that the bacterial sensory system is matched to the task that it is required to perform. Both excitation- and adaptation-related phenomena occur on a time scale of seconds. The initial events in signal processing are similar in wild-type cells and in cells unable to methylate or demethylate, or both; however, they are markedly different in cells carrying *cheZ* mutations.

Characteristics of the Wild-Type Response

The impulse response shown in Figure 3A has a substantial width; it persists for about 4 sec. This means that a cell integrates stimuli that have occurred over the past few seconds in determining its present bias: variations in concentration that occur on a time scale much shorter than this average out. This is characteristic of a low-pass filter, a device that passes low frequencies in preference to high frequencies. The impulse response also is biphasic; one lobe is above the baseline and the other is below it. This means that the cell is sensitive to changes in concentration that have occurred over the past few seconds: variations in concentration that occur on a time scale much longer than this also average out. This is characteristic of a differentiator, or high-pass filter, a device that is sensitive to changes in input—that is, that passes high frequencies in preference to low frequencies. If the areas of the two lobes are equal, the output returns to its initial value after a stepwise change in input, as illustrated in Figure 4; the device is fully adaptive. In summary, the impulse response has bandpass properties; the cell is maximally sensitive to frequencies at which the low-pass and high-pass contributions overlap.

We could carry this analysis further by exposing the cell to sinusoidal stimuli and measuring the amplitude of the resultant swings in rotational bias as a function of frequency. But this is not necessary, because an equivalent result is obtained by decomposing the impulse response into its spectral components by means of the Fourier transform (Papoulis, 1977). A Bode (log–log) plot of this spectrum, shown in Figure 8, shows the bandpass properties. The system has a maximum pass frequency at 0.25 Hz, corresponding to a time span of 4 sec. A decomposition of the system into constituent filters is done by matching the slopes on either side of the pass frequency. Positive slopes indicate high-pass characteristics, and negative slopes indicate low-pass characteristics. The steepness of the slope determines the sharpness of the frequency cutoff: an asymptotic slope of $20n$ dB/decade indicates an nth order filter. The wild-type sensory system behaves roughly as a first order high-pass filter in cascade with a third order low-pass filter.

The 4 sec bandpass time implies that the system is maximally sensitive to changes occurring with this periodicity. This bandpass covers the range of frequencies that a cell generates by its motion when

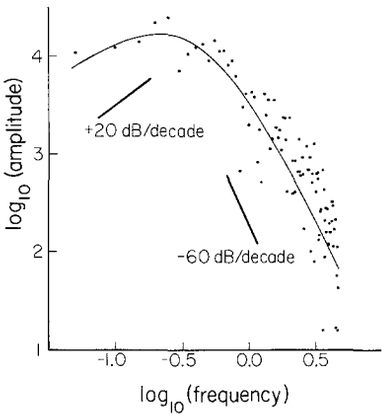

Figure 8. Fourier Transform of the Wild-Type Response

A Bode plot—$\log_{10}$(amplitude) versus $\log_{10}$(frequency)—of the absolute magnitude of the complex Fourier transform of the impulse response shown in Figure 3A. The transform peaks at approximately 0.25 Hz, corresponding to a bandpass centered at 4.0 sec. Slopes of +20 dB and −60 dB are shown for reference. The response system, if linear, is approximated by a first order high-pass filter in cascade with a third order low-pass filter. The response array of 1024 points was digitally filtered prior to transformation to reduce high-frequency contamination. Low-frequency trends were eliminated by subtracting out the baseline determined by a least-squares fit to the data obtained before and well after the response. The solid line is the transform of a nonlinear least-squares fit to the impulse response of a sum of four exponentials.

swimming in a spatial gradient. As we noted earlier, a swimming cell executes a random walk with steps (runs) averaging approximately 1 sec. The concentration rises and falls as the cell moves up and down the gradient; frequencies on the order of 0.25 Hz are prominent.

As noted above, the distributed nature of the impulse response indicates that cells make use of information over a time span extending at least 4 sec into the past. The Fourier analysis shows that they weight spectral components of stimuli with periods around 4 sec most heavily. Thus, while it can be said that a cell has "memory," it does not have a memory characterized by a single decay time. A time span of 2 sec is roughly equal to the persistence time of a cell swimming in a spatial gradient—that is, the mean time during which there is a component of cell motion up the gradient (Macnab and Koshland, 1973; Lovely and Dahlquist, 1975). This is another way of saying that the sensory system is optimized to sense those changes in concentration encountered when the cell swims in a gradient.

The question of memory time in bacterial chemotaxis has been addressed before. The long relaxation times for adaptation to steps in concentration imply a kind of "memory" in the limited sense that prior to adaptation, the cell continues to respond to a change made in the past (Macnab and Koshland, 1972). Adaptation times, however, are a function of the stimulus size (Spudich and Koshland, 1975; Berg and Tedesco, 1975) and do not point to a particular characteristic memory time, t_m. Memory is not "useful" if it extends so far into the past that the information retained is not relevant to the current trajectory of the cell (Macnab and Koshland, 1973). Computer simulations of cells swimming in a spatial gradient show that a long memory is clearly detrimental (Brown and Berg, 1974). For cells with a memory that decayed exponentially with a time constant t_m, the rate of drift up the gradient fell off exponentially with a time constant of the order of $2t_r$, where t_r is the mean run interval. For values of $t_m > 5t_r$, chemotaxis was essentially abolished.

Why should the mean run interval be about 1 sec? On the one hand, runs must be long enough to allow the cell to sense changes in concentration in the presence of random fluctuations (noise); the precision with which such changes can be sensed improves with the square root of the measurement time (Berg and Purcell, 1977). On the other hand, the runs must not be so long that the curvature induced by rotational Brownian movement causes the cell to deviate significantly from its path before the measurement is complete. For a cell the size of E. coli, this is a serious problem for times on the order of 10 sec (Brown and Berg, 1974). The mean run interval must be shorter than this, so that when favorable runs are extended, they still fall within this limit. Hence the optimum run interval is determined by these physical constraints.

Modulation of a Two-State System

Very little is known about the machinery that generates the impulse response, but it is known that the baseline behavior of the cell involves random switching between two rotational modes. The underlying events that terminate CCW and CW intervals have constant probabilities in time. The simplest model that has this property is a two-state system, in which the states dictate either CCW rotation (runs) or CW rotation (tumbles). These states might represent alternate configurations of a protein that determine the direction of rotation, the binding and unbinding of a ligand on such a protein, or the like. Transitions between the two states are governed by first order rate constants k_r and k_t, which are the probabilities per unit time of terminating a run or a tumble, respectively.

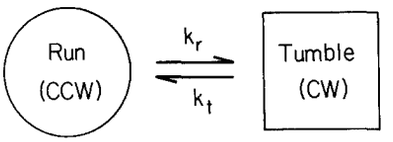

In this system CCW intervals are distributed as $\exp(-k_r t)$ and CW intervals are distributed as $\exp(-k_t t)$. If k_r is greater than k_t, the motor spends most of its time in the tumble mode; if k_t is greater than k_r, the run mode predominates. In general, if both k_r and k_t are large, the reversal rate is high; if both k_r

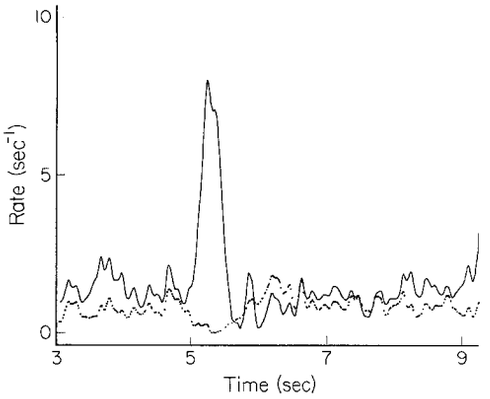

Figure 9. Rate Constants for the Two-State Model

The rate constants k_t (solid line) and k_r (dotted line) computed for the impulse response of Figure 3A and shown as a function of time. Note that k_r and k_t are anticorrelated during the positive phase of the impulse response, which lasts about 1 sec, as well as during the subsequent undershoot. The relatively high noise level reflects the large statistical variance in the reversal rate. This graph was prepared from the impulse response, its time derivative and the instantaneous reversal rate, as described in the text; see equations (3) and (4).

and k_t are small, the reversal rate is low. We suppose that the sensory system modulates k_r and k_t. The changes that occur during the impulse response can be derived from measurements of the probability of spinning CCW and the reversal rate, as outlined in Experimental Procedures. The results are shown in Figure 9. During the initial phase of the response, k_t rises and k_r drops. During the undershoot, k_r exceeds k_t, and tumbles are transiently favored. The response to a repellent gives essentially the same result, but with the roles of k_r and k_t interchanged (data not shown). If the cell actually works in this way, k_r and k_t must be controlled jointly by the sensory system, and they must be modulated in an antagonistic manner. If this modulation is to override the steady state reversal behavior, as implied by the results in Figure 5, the mechanism that controls the rate constants must act quite rapidly. Cells with different unstimulated biases (and different mean CCW and CW rotation intervals) give impulse responses with virtually identical time courses (data not shown). This suggests that the mechanism that controls the rate constants is quite similar from cell to cell, but distinct from the mechanism that sets the prestimulus values of these constants. The latter mechanism has a large biological variability (Berg and Tedesco, 1975; Spudich and Koshland, 1976).

Characteristics of Mutant Responses

It should be possible through the analysis of generally nonchemotactic mutants to work out the functions and interrelationships of different components of the signal-transduction pathway (see Parkinson, 1981; Boyd and Simon, 1982). One needs a combined assault with the use of genetics, biochemistry and physiology. Although a great deal has been learned with slower methods, our results show that important physiological events occur on a relatively short time scale: a time scale not accessible to those methods. Defects in some mutants are so severe that the cells fail to respond to any stimuli; these strains are not amenable to the analysis undertaken here. Fortunately, other *che* mutants do respond, to varying degrees, and we have begun by examining some of these.

The impulse response of cells with a *cheR–cheB* double deletion shown in Figure 7A is similar to that of wild-type cells (Figure 3A). It begins at roughly the same baseline, has essentially the same rise time and follows a similar time course for the first second or so, but it does not have as large an undershoot. As noted in the Results, this feature varied from cell to cell. The lack of a pronounced undershoot, on the average, for the mutant implies that it lacks some of the high-pass (adaptive) properties of the wild-type strain. This was confirmed through measurements of responses to small-step stimuli that unlike those for wild-type cells shown in Figure 4, failed to return to the baseline (in 10 sec, the longest period studied). These responses agreed with those predicted by convolution of a step stimulus with the mutant impulse response (data not shown).

The diminution in the undershoot is correlated with the absence of the enzymes that methylate and demethylate the MCPs. Therefore, it is likely that this aspect of the impulse response is caused by increased levels of methylation that accompany an increase in the concentration of attractant. This suggests that a transient burst of methylation initiated by the impulse feeds back in such a way as to depress the CCW bias.

We would expect these mutants to possess some chemotactic ability. As the cells move up a gradient, however, their CCW bias will become so great that the run intervals will soon exceed the limits of usefulness imposed by rotational Brownian movement (see above). In this limit, the cells will no longer be chemotactic. It is possible, at least in theory, to perform chemotaxis in the complete absence of adaptation. Runs up the gradient of an attractant will still be longer, and runs down will be shorter. In this case, however, chemotaxis will only be effective over a limited range in concentration, a range over which the rotational bias of the cell remains unsaturated and run lengths do not exceed the Brownian limit. Cells carrying *cheR–cheB* double deletions do, in fact, form chemotactic rings on soft agar containing tryptone (data not shown). These rings, although much smaller than those produced by wild-type cells, are substantially larger than swarms formed by completely nonchemotactic strains, such as *cheY* or *cheZ*. The possibility remains that the cells carrying *cheR–cheB* deletions are in fact adaptive, but only over a time span much longer than that probed by our measurements. (For examples of adaptation to other attrac-

tants not involving methylation, see Niwano and Taylor, 1982.)

Cells carrying mutations in either the *cheB* or *cheR* genes also have impulse responses that resemble that of the wild-type, at least for the first second or so (Figures 7C and 7D). The shape and duration of the first lobes are much the same, but any undershoot or overshoot is obscured by the baseline biases, which are almost exclusively CW or CCW, respectively. We conclude that the mechanisms responsible for generating the first lobe of the impulse response do not involve methylation or demethylation.

The *cheZ* mutants appear to be defective in excitation and to have a very long "memory time." The response shows a long rise time and a very slow recovery (Figure 7B). An undershoot, if it exists, did not develop on the time scale of our measurements. Short impulses of the kind used to stimulate wild-type cells had essentially no effect. Longer pulses (still short on the time scale of the response) set in motion a characteristic sequence of brief CCW bursts; some of these sequences lasted for many seconds. The response did not return to baseline, even 15 sec after the onset of a pulse. As noted earlier, a cell that averages temporal information with such a long time base cannot be chemotactic, because the older information is not relevant to the current trajectory. There exist *cheZ–cheC* double mutants that fail to move up gradients, even though their tumbling rates are normal (Parkinson and Parker, 1979). They are likely to be nonchemotactic both because of a slow response and because of an excessive memory time.

Preliminary measurements of responses of *cheZ* mutants to step stimuli did not agree with those predicted by convolution with the impulse response. The discrepancy might be due to long-range behavior occurring outside the time domain that we investigated, to a nonlinearity in the *cheZ* response or to the fact that the limited amount of step-stimulus data available was not representative of the population of *cheZ* cells as a whole. Further work on these mutants is in progress.

Epilogue

In a recent review, Boyd and Simon (1982) discussed the implications of evolution for chemotaxis. They suggested that chemotaxis initially arose as a response to a transient change in the cellular state (such as perturbation of pH or protonmotive force). Cellular mechanisms of homeostasis restored that state, thus providing a primitive form of adaptation within a limited range. Other mechanisms of adaptation, involving methylation, developed later, allowing adaptation to occur over a wider dynamic range. The components of this system then became sensitive to specific sensory inputs. Our data on responses to aspartate are consistent with this view. Even without methylation or demethylation, E. coli has the ability to integrate information over lengths of time comparable with the duration of a run and has a limited capacity to adapt. The imperfections inherent in this process might have been compensated for by the development of a system that restores the rotational bias of the motor, so that a cell that has drifted up a gradient remains able to respond. Reversible carboxymethylation of the MCPs might provide a basis for such a system, with the primary function of range adjustment. In any event, it is clear from our results that E. coli contains sophisticated machinery for chemotaxis. This machinery processes sensory information over a time span of a few seconds, making maximal use of the information available. The iontophoretic technique provides a means of defining the physiological properties of mutants with defects in this machinery, and thus of learning more about how signal transduction works.

Experimental Procedures

Chemicals

α-Methyl-D,L-aspartate and D,L-leucine were obtained from Sigma; other L-amino acids (A grade) were obtained from Calbiochem; nickel chloride was obtained from Fisher; benzoic and lactic acids (reagent grade) were obtained from Mallinckrodt; and thorium chloride was obtained from ICN-K&K Pharmaceuticals. Tetraethylpentamine (tetren; technical grade) was obtained from Aldrich and purified according to the method of Reilley and Vavoulis (1959).

Bacterial Strains

The wild-type strain was AW405, an E. coli K12 derivative auxotrophic for threonine, leucine and histidine, obtained from J. Adler (Armstrong et al., 1967). Mutant strains were: *cheR* deletion, RP4968; *cheB* deletion, RP4972; *cheR–cheB* double deletions, RP1273 (Sherris and Parkinson, 1981), RP4969, RP4970; *cheZ* point mutants, RP5007 (*cheZ293*) and RP5008 (*cheZ278*) (Parkinson, 1978). All *che* mutants were provided by J. S. Parkinson.

Preparation of Tethered Cells

Cells were grown to saturation in a minimal growth medium containing glycerol and essential amino acids (Hazelbauer et al., 1969), diluted 1:100 and grown again in the same medium, and harvested at mid-exponential phase. The cells were grown at 35°C in a rotary incubator; collected by centrifugation; washed once or twice in a motility medium containing 90 mM NaCl, 10 mM KCl, 10 mM Tris–Cl (pH 7.0 at 32°C), 10 mM sodium lactate, 0.1 mM tetren and 0.001 mM methionine; and resuspended in this medium at one-fifth the original volume. The cells were sheared by passage of this suspension 60 times between two syringes equipped with 26-gauge needles connected with an 8 cm length of polyethylene tubing (0.58 mm internal diameter). The cells were washed twice more, and tethered to a coverslip as described by Berg and Tedesco (1975).

Data Acquisition

The coverslip to which the cells were tethered was sealed to the bottom of a stainless-steel chamber mounted on the stage of a phase-contrast microscope. The cells were viewed through a 40× water-immersion objective (Zeiss). Both the stage and the objective were heated to 32.0°C. The objective was thermally and electrically isolated from the microscope body. The preparation was slowly perfused with motility medium during the entire experiment. Iontophoretic pipettes filled with motility medium containing 0.01 mM thorium chloride and either attractants or repellents were prepared as described by Segall et al. (1982). Pipette resistances were 15–50 megohms. A current-injection circuit (Dreyer and Peper, 1974) was used to pass current (1–200 nA) through the pipettes via Ag/AgCl wires. Control experiments, in which no attractant or repellent was added to the

medium in the pipettes, yielded no response (Segall et al., 1982). The microscope was equipped with an optoelectronic device that extracts the x and y coordinates of the centroid of the image of a spinning cell, $x = \sin(\omega t)$ and $y = \sin(\omega t \pm \phi)$, where ω is the angular velocity of the cell and ϕ is a 90° phase shift, the sign of which indicates the handedness of the rotation (apparatus of Kobayasi et al., 1977, as modified by Berg et al., 1982). Cells that were monitored with this device met several criteria: they were tethered around a point near one end; they rotated with a regular, circular motion; their center of rotation did not change appreciably when they underwent reversals; and their angular velocity was between 5 and 12 Hz. Cells were stimulated about once a minute. Records of the x and y coordinates were made on a strip-chart recorder (Gould Brush 220; run at 25 mm/sec), together with event markers indicating the sign of ϕ and the timing of the stimulus current, as illustrated in Figure 1 of Segall et al. (1982). The positions of the phase discontinuities, evident in the x and/or y signals, were digitized with a strip-chart digitizer built for the purpose. The data, a list of numbers representing the times of CW-to-CCW or CCW-to-CW transitions, measured relative to the onset of the stimulus, were stored as records in a PDP 11/34 computer for subsequent analysis. These numbers were accurate to within about 55 msec, with errors arising from delays due to the electronics, from uncertainties in the positions of the phase discontinuities on the strip-chart records or from random slippage of the paper in the digitizing apparatus.

Data Analysis

Over 1700 records, containing more than 35,000 events, were digitized in all. An array of computer programs was developed to collate, analyze and display data reduced from these records. Each record contained a list of numbers corresponding to the times at which reversals in the direction of rotation occurred. A chronological list of all such numbers in a set of n records was compiled by concatenating the records and sorting the numbers with the Shell-Metzner algorithm (see, for example, Wirth, 1976). A function was constructed whose initial value was taken to be equal to the total number of records in which the cell was spinning CCW at time zero. The value of the function for subsequent times was computed by changing the previous value by unity at every reversal: +1 for a CW-to-CCW transition, −1 for a CCW-to-CW transition. An estimate of the probability of spinning CCW was obtained by dividing all the values in this function by n (Figure 1). Prior to display, this probability function was passed to a cubic spline-fit smoothing routine (Reinsch, 1967, 1971), which fits an array of cubic segments to the data. The endpoints of each segment are constrained to pass close to (but not necessarily through) the data, in such a way that the spline-fit curve fits the data in a least-squares sense. A smoothing parameter, specifying a χ^2 measure of the fit, governs the degree of smoothing. The routine was used to smooth data and to perform interpolation (see below).

The (uneven) density of points along the time axis in the probability function provided a measure of the total number of reversals occurring in the group of records at any instant. The average number of reversals per second per cell is this density divided by n. The density was computed by counting the total number of events up to a given time, and treating that number as a function of time. The time derivative (slope) of this curve gives the density of reversals. The derivative was computed by fitting the function with cubic splines, the coefficient of the linear term for each cubic giving the derivative. Smoothing was used to eliminate discontinuities in the density function.

The two-state model described in the text can be solved to give the fraction of time that a cell runs, f_r, and the reversal rate, ρ. When the system is at equilibrium, one obtains $f_r = k_t/(k_r + k_t)$ and $\rho = 2k_rk_t/(k_r + k_t)$. Even when the system is out of equilibrium, these quantities can be derived from a knowledge of f_r, its time derivative, df_r/dt, and ρ. Since

$$df_r/dt = -k_r f_r + k_t(1 - f_r) \tag{1}$$

and

$$\rho = k_r f_r + k_t(1 - f_r), \tag{2}$$

it follows that

$$k_r = \frac{\rho - df_r/dt}{2f_r} \tag{3}$$

and

$$k_t = \frac{\rho + df_r/dt}{2(1 - f_r)}. \tag{4}$$

The rate constants in Figure 9 were calculated according to equations (3) and (4) with the use of the impulse response, its time derivative and the reversal rate. The impulse response and reversal rate were determined as previously described. The time derivative of the impulse response was obtained from the cubic spline-fit to the rotational data by a method similar to that described for the reversal rate. Both the reversal rate and the impulse response data were smoothed prior to the computation; no smoothing was performed on the result.

The Fourier transform of the impulse response was performed on an array of 1024 points with a Fast Fourier Transform Module (Digital Equipment Corporation). The magnitude of the transform was computed from the real and complex parts. The input array of equally spaced points was obtained by interpolation of 400 unevenly spaced points from Figure 3A with the cubic spline-fit smoothing routine. Some smoothing was done to eliminate excessive noise at high frequencies. Low-frequency trends were eliminated by choosing a baseline and subtracting out the best-fit straight line prior to transformation. Aliasing was reduced by choosing the length of the transformed record (20 sec) to be close to an integral multiple of the impulse response period (approximately 4 sec).

The predicted response to a small step was computed by a routine that performs the convolution integral of an experimentally determined impulse response with a step function of adjustable amplitude. The impulse response was interpolated and smoothed as described above, and the integration was carried out numerically by Romberg extrapolation (Acton, 1970).

Acknowledgments

S. M. B. and J. E. S. contributed equally to the work. We are grateful to Robert Smyth for discussion and for providing computer routines. We also thank Markus Meister for theoretical contributions to the two-state model, and Paul Meyer for discussion of small-step stimuli. This work was supported by a grant from the National Institute of Allergy and Infectious Diseases. J. E. S. acknowledges support as an NSF predoctoral fellow.

The costs of publication of this article were defrayed in part by the payment of page charges. This article must therefore be hereby marked "*advertisement*" in accordance with 18 U.S.C. Section 1734 solely to indicate this fact.

Received July 13, 1982

References

Acton, F. S. (1970). Numerical Methods That Work. (New York: Harper & Row), pp. 100–129.

Armstrong, J. B., Adler, J. and Dahl, M. M. (1967). Nonchemotactic mutants of *Escherichia coli*. J. Bacteriol. *93*, 390–398.

Berg, H. C. and Brown, D. A. (1972). Chemotaxis in *Escherichia coli* analysed by three-dimensional tracking. Nature *239*, 500–504.

Berg, H. C. and Purcell, E. M. (1977). Physics of chemoreception. Biophys. J. *20*, 193–219.

Berg, H. C. and Tedesco, P. M. (1975). Transient response to chemotactic stimuli in *Escherichia coli*. Proc. Nat. Acad. Sci. USA *72*, 3235–3239.

Berg, H. C., Manson, M. D. and Conley, M. P. (1982). Dynamics and energetics of flagellar rotation in bacteria. Symp. Soc. Exp. Biol. *35*, 1–31.

Boyd, A. and Simon, M. (1980). Multiple electrophoretic forms of methyl-accepting chemotaxis proteins generated by stimulus-elicited methylation in *Escherichia coli*. J. Bacteriol. *143*, 809–815.

Boyd, A. and Simon, M. (1982). Bacterial chemotaxis. Ann. Rev. Physiol. *44,* 501–517.

Brown, D. A. and Berg, H. C. (1974). Temporal stimulation of chemotaxis in *Escherichia coli.* Proc. Nat. Acad. Sci. USA *71,* 1388–1392.

Chelsky, D. and Dahlquist, F. W. (1980). Structural studies of methyl-accepting chemotaxis proteins of *Escherichia coli*: evidence for multiple methylation sites. Proc. Nat. Acad. Sci. USA *77,* 2434–2438.

DeFranco, A. L. and Koshland, D. E., Jr. (1980). Multiple methylation in processing of sensory signals during bacterial chemotaxis. Proc. Nat. Acad. Sci. USA *77,* 2429–2433.

Dreyer, F. and Peper, K. (1974). Iontophoretic application of acetylcholine: advantages of high resistance micropipettes in connection with an electronic current pump. Pflügers Arch. ges. Physiol. *348,* 263–272.

Engström, P. and Hazelbauer, G. L. (1980). Multiple methylation of methyl-accepting chemotaxis proteins during adaptation of E. coli to chemical stimuli. Cell *20,* 165–171.

Goy, M. F., Springer, M. S. and Adler, J. (1977). Sensory transduction in *Escherichia coli*: role of a protein methylation reaction in sensory adaptation. Proc. Nat. Acad. Sci. USA *74,* 4964–4968.

Goy, M. F., Springer, M. S. and Adler, J. (1978). Failure of sensory adaptation in bacterial mutants that are defective in a protein methylation reaction. Cell *15,* 1231–1240.

Hazelbauer, G. L., Mesibov, R. E. and Adler, J. (1969). *Escherichia coli* mutants defective in chemotaxis toward specific chemicals. Proc. Nat. Acad. Sci. USA *64,* 1300–1307.

Kihara, M. and Macnab, R. M. (1981). Cytoplasmic pH taxis and weak-acid repellent taxis of bacteria. J. Bacteriol. *145,* 1209–1221.

Kobayasi, S., Maeda, K. and Imae, Y. (1977). Apparatus for detecting rate and direction of rotation of tethered bacterial cells. Rev. Sci. Instr. *48,* 407–410.

Kondoh, H., Ball, C. B. and Adler, J. (1979). Identification of a methyl-accepting chemotaxis protein for the ribose and galactose chemoreceptors of *Escherichia coli.* Proc. Nat. Acad. Sci. USA *76,* 260–264.

Kort, E. N., Goy, M. F., Larsen, S. H. and Adler, J. (1975). Methylation of a membrane protein involved in bacterial chemotaxis. Proc. Nat. Acad. Sci. USA *72,* 3939–3943.

Koshland, D. E., Jr. (1981). Biochemistry of sensing and adaptation in a simple bacterial system. Ann. Rev. Biochem. *50,* 765–782.

Larsen, S. H., Reader, R. W., Kort, E. N., Tso, W.-W. and Adler, J. (1974). Change in direction of flagellar rotation is the basis of the chemotactic response in *Escherichia coli.* Nature *249,* 74–77.

Lovely, P. S. and Dahlquist, F. W. (1975). Statistical measures of bacterial motility and chemotaxis. J. Theor. Biol. *50,* 477–496.

Macnab, R. M. (1978). Bacterial motility and chemotaxis: the molecular biology of a behavioral system. CRC Crit. Rev. Biochem. *5,* 291–341.

Macnab, R. M. and Koshland, D. E., Jr. (1972). The gradient-sensing mechanism in bacterial chemotaxis. Proc. Nat. Acad. Sci. USA *69,* 2509–2512.

Macnab, R. and Koshland, D. E., Jr. (1973). Persistence as a concept in the motility of chemotactic bacteria. J. Mechanochem. Cell. Motil. *2,* 141–148.

Marmarelis, P. Z. and Marmarelis, V. Z. (1978). Analysis of Physiological Systems. (New York: Plenum), pp. 11–130.

Niwano, M. and Taylor, B. L. (1982). Novel sensory adaptation mechanism in bacterial chemotaxis to oxygen and phosphotransferase substrates. Proc. Nat. Acad. Sci. USA *79,* 11–15.

Papoulis, A. (1977). Signal Analysis. (New York: McGraw-Hill), pp. 3–25, 56–138.

Parkinson, J. S. (1978). Complementation analysis and deletion mapping of *Escherichia coli* mutants defective in chemotaxis. J. Bacteriol. *135,* 45–53.

Parkinson, J. S. (1981). Genetics of bacterial chemotaxis. Symp. Soc. Gen. Microbiol. *31,* 265–290.

Parkinson, J. S. and Parker, S. R. (1979). Interaction of the *cheC* and *cheZ* gene products is required for chemotactic behavior in *Escherichia coli.* Proc. Nat. Acad. Sci. USA *76,* 2390–2394.

Parkinson, J. S. and Revello, P. T. (1978). Sensory adaptation mutants of E. coli. Cell *15,* 1221–1230.

Reilley, C. N. and Vavoulis, A. (1959). Tetraethylenepentamine, a selective titrant for metal ions. Anal. Chem. *31,* 243–248.

Reinsch, C. H. (1967). Smoothing by spline functions. Numerische Mathematik *10,* 177–183.

Reinsch, C. H. (1971). Smoothing by spine functions II. Numerische Mathematik *16,* 451–454.

Segall, J. E., Manson, M. D. and Berg, H. C. (1982). Signal processing times in bacterial chemotaxis. Nature *296,* 855–857.

Sherris, D. and Parkinson, J. S. (1981). Posttranslational processing of methyl-accepting chemotaxis proteins in *Eshcerichia coli.* Proc. Nat. Acad. Sci. USA *78,* 6051–6055.

Silverman, M. and Simon, M. (1974). Flagellar rotation and the mechanism of bacterial motility. Nature *249,* 73–74.

Silverman, M. and Simon, M. (1977). Chemotaxis in *Escherichia coli*: methylation of *che* gene products. Proc. Nat. Acad. Sci. USA *74,* 3317–3321.

Springer, M. S., Goy, M. F. and Adler, J. (1977). Sensory transduction in *Escherichia coli*: two complementary pathways of information processing that involve methylated proteins. Proc. Nat. Acad. Sci. USA *74,* 3312–3316.

Springer, M. S., Goy, M. F. and Adler, J. (1979). Protein methylation in behavioral control mechanisms and in signal transduction. Nature *280,* 279–284.

Springer, W. R. and Koshland, D. E., Jr. (1977). Identification of a protein methyltransferase as the *cheR* gene product in the bacterial sensing system. Proc. Nat. Acad. Sci. USA *74,* 533–537.

Spudich, J. L. and Koshland, D. E., Jr. (1975). Quantitation of the sensory response in bacterial chemotaxis. Proc. Nat. Acad. Sci. USA *72,* 710–713.

Spudich, J. L. and Koshland, D. E., Jr. (1976). Non-genetic individuality: chance in the single cell. Nature *262,* 467–471.

Stock, J. B. and Koshland, D. E., Jr. (1978). A protein methylesterase involved in bacterial sensing. Proc. Nat. Acad. Sci. USA *75,* 3659–3663.

Tsang, N., Macnab, R. and Koshland, D. E., Jr. (1973). Common mechanism for repellents and attractants in bacterial chemotaxis. Science *181,* 60–63.

Wirth, N. (1976). Algorithms + Data Structures = Programs. (Englewood Cliffs, N. J.: Prentice-Hall), pp. 56–124.